

# Supporting Information

Boughton et al. 10.1073/pnas.1108236108

## SI Text

**Materials and Sample Preparation. Protein preparation.** Samples of bovine GRK2 and geranylgeranylated G $\beta\gamma$  were expressed in baculovirus-infected cell culture, purified as previously described, and frozen in liquid nitrogen (1). In order to determine whether or not the spectra at the interface originated from the bound GRK2-G $\beta\gamma$  complex, the G $\beta\gamma$ -binding deficient mutant GRK2-R587Q was similarly prepared from virus obtained from J. Benovic (Thomas Jefferson University) (2). Using a flow cytometry protein interaction assay (3), we confirmed that GRK2-R587Q does not bind G $\beta\gamma$  under conditions that wild-type GRK2 binds with a  $K_D$  of 50 nM. A complex containing both GRK2 and G $\beta\gamma$  was isolated off S200 size exclusion columns from protein isolated from cells that were coinfecting with baculoviruses encoding the G $\beta_1$ , G $\gamma_2$ , and GRK2 proteins. On the day of experiments, protein aliquots were thawed and centrifuged through Nanosep MF 0.2  $\mu$ m filters (Pall Corporation) to remove aggregated protein, and the concentration was calculated by  $A_{280}$ . Samples were diluted directly into a solution containing 20 mM Hepes (pH 8.0), 50 mM NaCl, and 5 mM DTT. This buffer mixture was also used as the liquid subphase for the lipid bilayer.

**Bilayer preparation.** Planar supported lipid bilayers (PSLBs) were prepared as model membranes, using the Langmuir-Blodgett / Langmuir-Schaefer deposition method as described previously (4). To model the composition of mammalian cell membranes, a 9:1 mixture of POPC/POPG lipids was used. Lipids were purchased from Avanti Polar Lipids Inc., dissolved in chloroform, and mixed as needed to produce the desired lipid mixture composition. Following bilayer creation, the bilayer subphase was flushed three times with fresh buffer to remove excess lipids prior to addition of the protein. All samples were prepared on clean right-angle CaF<sub>2</sub> prism substrates (Altos Photonics, Bozeman, MT) and SFG spectra were collected from the proteins associated with the lipid bilayer in a total internal reflection geometry (5).

**Data Analysis and Interpretation. Defining the reference orientation.** In this work, all data analysis is described in terms of a reference orientation, which for convenience refers to the expected position of the GRK2-G $\beta\gamma$  complex when interacting with the membrane. The reference orientation was defined using the C $\alpha$  atoms of residues in the complex that are expected to be involved in membrane-protein interactions. Protein Data Bank (PDB) entry 1omw was then rotated so that a plane through these residues would coincide with the membrane plane. The Pymol atom selection used for the linear-least-squares plane fitting procedure was as follows:

```
cmd.select ["membres_complex", "name ca and (chain A and (resi 30-31 or resi 209 or resi 528-547 or resi 569-576) ) or (chain B and (resi 46 or resi 48) ) or (chain G and (resi 62 or resi 66-68)) "]
```

**Graphical depiction of physically allowed orientations.** Although Euler angles provide an efficient way to perform rotations, the resulting combinations of tilt and twist angles depicted in the results of this paper are not always straightforward to visualize. Furthermore, not all mathematically allowed solutions are in fact physically reasonable given restraints such as geranylgeranylation, or the possibility of atoms colliding with the membrane. We have produced an overlay layer (Fig. S1) that can be added to experimental measurements (Fig. 4, main text) to better indicate which combinations of tilt and twist angle are physically

meaningful. This overlay was produced using a Pymol script that assigned all orientations a binary “allowed/disallowed” score. The criterion presented in this work was kept as simple as possible: physically allowed positions were defined as those where less than 10% of the backbone  $\alpha$  carbons collided with the membrane. Because it is known that the geranylgeranyl group of G $\beta\gamma$  plays a key role in anchoring the protein to the membrane, this criterion was thus implemented by accepting all positions where less than 10% of backbone atoms were below the c-terminal residue of the G $\gamma$  chain. (the geranylgeranyl attachment point).

**The effect of choosing alternate assumed initial positions of the complex to determine G $\beta\gamma$  orientation.** In this work, we describe a method of orientation analysis that uses two experimental measurements to reveal the allowed orientations of the G $\beta\gamma$  subunit, provided that the initial orientation of the complex is known. As described above, the reference membrane was assigned via linear least-squares fitting of a plane passing through known membrane interacting residues. However, the calculated  $\frac{\chi_{zzz}^{(2)}}{\chi_{xxz}^{(2)}}$  ratio did not match the experimentally measured value at this position, indicating that the actual orientation is somewhat different. If we assume that the membrane interacting surface is not substantially curved, and that the known membrane orientation is dictated by the geranylgeranyl anchoring group, then a very good match for the experimentally measured ppp/ssp ratio can be achieved by assuming that the complex adopts a small tilt (at the position  $\theta = 10^\circ$ ,  $\psi = 180^\circ$ , as assumed in the paper).

However, other physically allowed orientations of the complex can also produce the expected  $\chi_{zzz}^{(2)}$  ratio. At these alternate positions of the complex, the calculated value of  $\chi_{xxz}^{(2)}$  may be different from the value assumed in this work. This difference would in turn affect the measurement of the signal intensity change upon complex formation, by altering the value of  $\chi_{\text{complex}}$  (determined by fitting the spectra) in the denominator of  $\frac{\chi_{G\beta\gamma,xxz}^{(2)}(\theta,\psi)}{\chi_{\text{complex},xxz}^{(2)}(\theta_{\text{fixed}},\psi_{\text{fixed}})}$ .

Fig. S24 shows the values of  $\chi_{xxz}^{(2)}$  for the GRK2-G $\beta\gamma$  complex at all of the positions that match within  $+/- 10\%$  of the experimentally measured  $\frac{\chi_{zzz}^{(2)}}{\chi_{xxz}^{(2)}}$  ratio for the complex (one measurement), subject to the additional constraint that the possible matches are physically reasonable orientations (as determined above). No scoring is applied, and the color values in Fig. S24 indicate the value of  $\chi_{\text{complex},xxz}^{(2)}$  at that point. Insofar as the drop in signal upon formation of the GRK2-G $\beta\gamma$  complex depends on the numerical value  $\chi_{\text{complex},xxz}^{(2)}$ , then the search space for use in the intensity/fitted signal strength change measurement only requires using different values for  $\chi_{\text{complex},xxz}^{(2)}$  in the denominator. The use of a specific value of  $\chi_{\text{complex},xxz}^{(2)}$  is much simpler than trying every possible position of the GRK2-G $\beta\gamma$  complex when choosing a fixed, known orientation of the complex. Because many of the allowed orientations of the complex would generate similar SFG signal, the ratio of signals from the two samples does not have to be calculated for all 32,400 points on the  $360^\circ$  by  $90^\circ$  plot representing angles of interest. Rather, the comparison of intensities need only be performed for the relatively small number of different values of  $\chi_{\text{complex},xxz}^{(2)}$ . The data analysis is then greatly simplified, which makes it possible to show whether G $\beta\gamma$  reorients

upon complex formation- even if the assumed orientation of the complex is slightly different from the actual orientation.

In order to determine which contour lines representing similar intensity are of greatest interest, the values depicted in Fig. S2A were histogrammed (Fig. S2B).

In Fig. S3, the effect of a change in the assumed position of the complex is explored. Each box shows the results from the second method of orientation analysis, in which allowed positions of G $\beta\gamma$  are indicated by considering which positions match experimental measurements when one particular value of  $\chi_{xxz}^{(2)}$  is assumed for the overall GRK2-G $\beta\gamma$  complex.

From Fig. S3, it is apparent that for  $\chi_{\text{complex},xxz}^{(2)} < 30$  or  $\chi_{\text{complex},xxz}^{(2)} > 120$ , all possible matches become either low scoring or nonexistent. Thus, the most likely positions of the complex are those that lie along a contour line within that range (such as the revised membrane orientation proposed in our paper). Our measurements indicate that the signals from G $\beta\gamma$  should be stronger than the signals obtained for GRK2-G $\beta\gamma$ , and this becomes harder to achieve as the value of  $\chi_{\text{complex},xxz}^{(2)}$  increases. Across this

subset of images shown, it may be seen that the most likely positions of G $\beta\gamma$  do shift somewhat as the assumed position of the complex is varied. In all cases, there is practically no overlap between the original assumed position of the complex and the final allowed positions of G $\beta\gamma$ . At best, the points where G $\beta\gamma$  does not reorient upon binding GRK2 have scores no greater than 60–80%, and those positions would result in less optimal contacts with the lipid bilayer. Thus we conclude that even if the actual position of the complex is slightly different than that assumed in the article, the conclusion that G $\beta\gamma$  likely reorients upon binding GRK2 would be qualitatively unchanged.

**Visual analysis of each separate constraint.** One goal of this research was to determine whether or not G $\beta\gamma$  reoriented upon formation of the GRK2-G $\beta\gamma$  complex. Depending on the choice of assumptions, either three or two measurements can be used, along with the overlay depicting physically allowed positions. The orientations that correspond to each separate constraint are presented here for completeness. (Fig. S4)

1. Lodowski DT, et al. (2003) Purification, crystallization and preliminary X-ray diffraction studies of a complex between G protein-coupled receptor kinase 2 and G $\beta 1\gamma 2$ . *Acta Crystallogr, Sect D: Biol Crystallogr* 59:936–939.
2. Carman CV, et al. (2000) Mutational analysis of G $\beta\gamma$  and phospholipid interaction with G protein-coupled receptor kinase 2. *J Biol Chem* 275:10443–10452.
3. Shankaranarayanan A, et al. (2008) Assembly of high order G $\alpha\alpha$ -effector complexes with RGS proteins. *J Biol Chem* 283:34923–34934.
4. Chen X, Chen Z (2006) SFG studies on interactions between antimicrobial peptides and supported lipid bilayers. *Biochim Biophys Acta* 1758:1257–1273.
5. Wang J, et al. (2003) Detection of Amide I signals of interfacial proteins in situ using SFG. *J Am Chem Soc* 125:9914–9915.

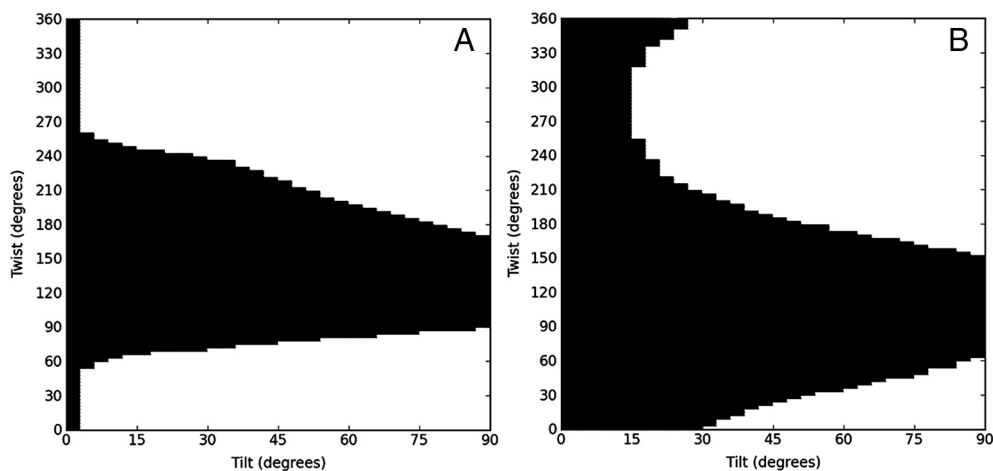


**Fig. 51.** Orientation angles corresponding to physically reasonable orientations of (A) the GRK2-G $\beta\gamma$  complex, or (B) G $\beta\gamma$  alone. These positions are indicated in black.



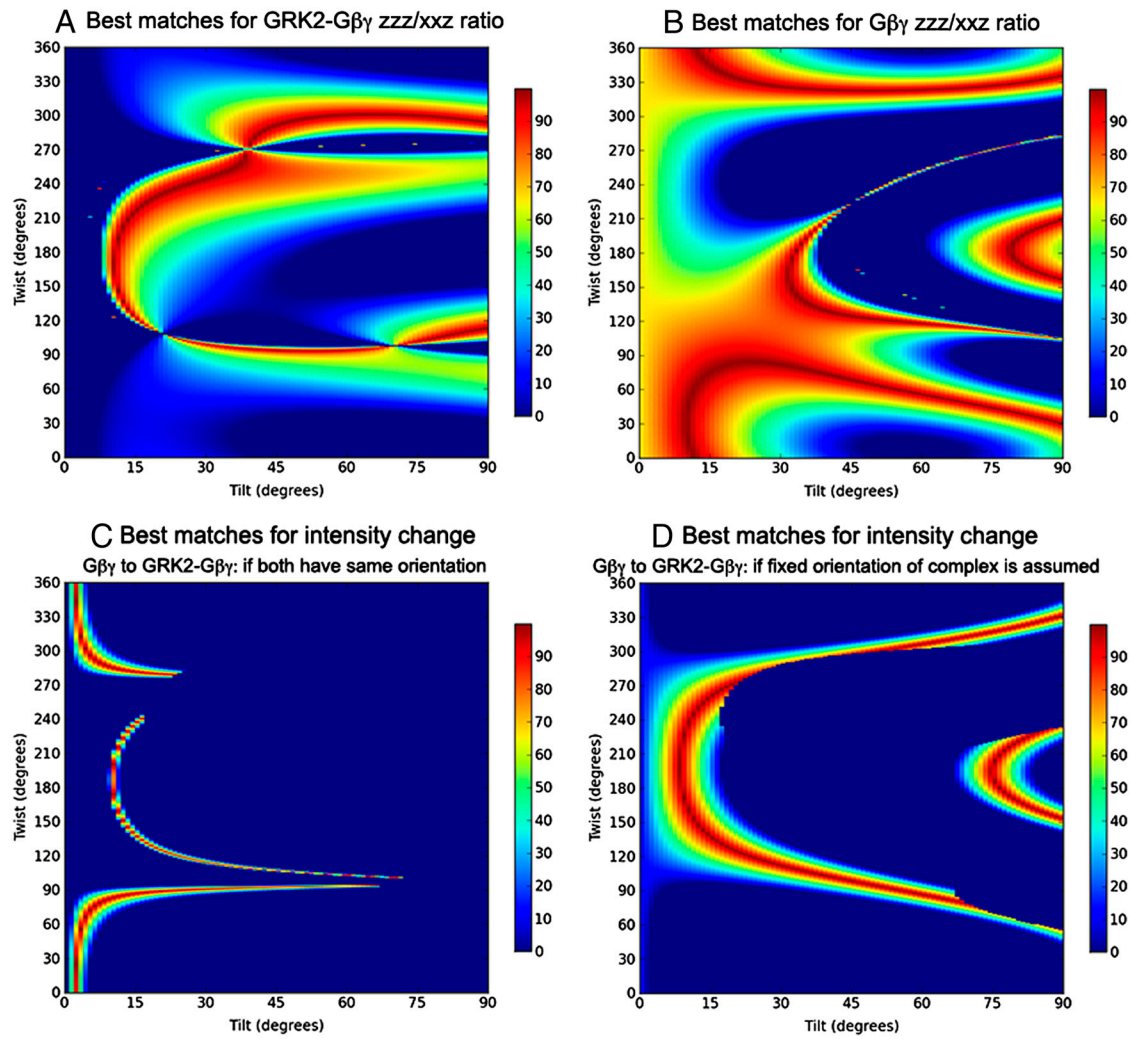


**Fig. S4.** Best matches for each separate experimental measurement. In box (D), the GRK2-G $\beta\gamma$  complex is assumed to adopt a single fixed orientation of tilt = 10°, twist = 180° relative to the reference position. The combination of boxes A–C results in Fig 4C of the main article. The combination of (B) and (D) results in Fig. 4D of the main article.